

Supporting information for

Title: Studying the cellular distribution of highly phototoxic platinated metalloporphyrins using isotope labelling

Authors: Riccardo Rubbiani,^{1#} Wenyu Wu,^{1#} Anu Naik,^{1#} Michele Larocca,¹ Lukas Schneider,¹ Roxane Padrutt,¹ Vipin Babu,¹ Christiane König,² Doris Hinger,³ Caroline Maake,³ Stefano Ferrari,^{2,5} Gilles Gasser,⁴ Bernhard Spingler^{1*}

Affiliations: ¹Department of Chemistry, University of Zurich, CH 8057 Zurich, Switzerland. ²Institute of Molecular Cancer Research, University of Zurich, Winterthurerstrasse 190, CH 8057 Zurich, Switzerland. ³Institute of Anatomy, University of Zurich, Winterthurerstrasse 190, CH 8057 Zurich, Switzerland. ⁴Chimie ParisTech, PSL University, CNRS, Institute of Chemistry for Life and Health Sciences, Laboratory for Inorganic Chemical Biology, F-75005 Paris, France. ⁵Institute of Molecular Genetics, Academy of Sciences of the Czech Republic, Videnska 1083, 143 00, Prague, Czech Republic.

the authors have contributed equally to the work

* To whom correspondence should be addressed. E-mail: spingler@chem.uzh.ch

Content:

Synthetic procedures to yield platinumated porphyrins **tPt-Zn4PyP**, **tPt-Cu4PyP**, **cPt-Zn4PyP**, **cPt-Cu4PyP**, **dPt-Zn4PyP**, **dPt-Cu4PyP** and **tPt-Py**. Singlet oxygen quantum yield determination.

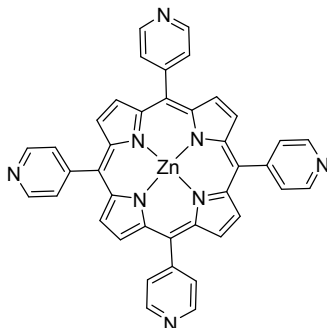
- Table S1: Crystal data of [*trans*-PtCl(NH₃)₂]₄-5,10,15,20-tetra(4'-pyridyl)-zinc(II)porphyrin tetraphenylborate · 7 DMF
- Table S2: Optimisation of the zinc(II) insertion into 5,10,15,20-tetra-(4'-pyridyl)-porphyrin
- Table S3: Singlet oxygen quantum yields (Φ_{Δ}) of **tPt-H₂4PyP**, **cPt-H₂4PyP**, **tPt-Zn4PyP** and **cPt-Zn4PyP** determined by the direct method in D₂O with irradiation at 420 nm
- Table S4: Pt and ⁶⁷Zn taken up in the different compartments of HeLa cells treated for 4 h at 10 μM with porphyrin **tPt-⁶⁷Zn4PyP**; results expressed in a) nmol metal / mg protein and b) in ng metal / mg protein
- Fig. S1: Reaction mechanism of the platinumation of a guanine nucleobase by platinumated porphyrins
- Fig. S2: Reaction of *trans*-[Pt(NH₃)₂(pyridine)Cl]NO₃ (**tPt-Py**) with guanosine
- Fig. S3: Overview of the 65 recorded ¹H-NMR spectra of **tPt-Py** reacting with one equivalent of guanosine in a 1:1 DMF-d₇:D₂O mixture
- Fig. S4: Inverse of the concentration vs. time plot for the signal at 5.95 ppm of the reaction of **tPt-Py** with guanosine in a 1:1 DMF-d₇:D₂O mixture
- Fig. S5: HR-MS-ESI of 5,10,15,20-tetra-(4'-pyridyl)-⁶⁷Zn(II)porphyrin (**⁶⁷Zn4PyP**)
- Fig. S6: UV-Vis of 5,10,15,20-tetra-(4'-pyridyl)-⁶⁷Zn(II)porphyrin (**⁶⁷Zn4PyP**) in DMF
- Fig. S7: HR-ESI-MS of [*trans*-PtCl(NH₃)₂]₄-5,10,15,20-tetra-(4'-pyridyl)-⁶⁷Zn(II)porphyrin nitrate (**tPt-⁶⁷Zn4PyP**)
- Fig. S8: ¹H-NMR of [*trans*-PtCl(NH₃)₂]₄-5,10,15,20-tetra-(4'-pyridyl)-⁶⁷Zn(II)porphyrin nitrate (**tPt-⁶⁷Zn4PyP**) in DMF
- Fig. S9: ¹³C-NMR of [*trans*-PtCl(NH₃)₂]₄-5,10,15,20-tetra-(4'-pyridyl)-⁶⁷Zn(II)porphyrin nitrate (**tPt-⁶⁷Zn4PyP**) in DMF
- Fig. S10: ¹⁹⁵Pt-NMR of [*trans*-PtCl(NH₃)₂]₄-5,10,15,20-tetra-(4'-pyridyl)-⁶⁷Zn(II)porphyrin nitrate (**tPt-⁶⁷Zn4PyP**) in DMF
- Fig. S11: UV-Vis of **tPt-H₂4PyP**, **tPt-Zn4PyP**, **cPt-H₂4PyP**, **cPt-Zn4PyP**, **dPt-H₂4PyP**, **dPt-Zn4PyP** in DMF
- Fig. S12: Example of ⁶⁷zinc calibration curve in ICP-MS and quantification lines in no gas mode
- Fig. S13: Ratio of intra- and extracellular content of ⁶⁷Zn and Pt after treatment of HeLa cells with **tPt-⁶⁷Zn4PyP**
- Fig. S14: ⁶⁷Zn and Pt biodistribution between nucleus and cytoplasmic fractions after treatment of HeLa cells with **tPt-⁶⁷Zn4PyP**
- Fig. S15: Characterization of DNA damage by γH2AX induced upon light activation of the photosensitizer **tPt-H₂4PyP**

Experimental Section:

The chemicals were purchased from Acros Organics (Belgium), Chempur (Germany), Fluorochem (United Kingdom) and Sigma-Aldrich (Switzerland). ⁶⁷Zinc as a metal was obtained from ISOFLEX USA (enrichment level of 89.6%). The solvents used in analysis were of reaction grade and purchased from EMSURE, the remaining solvents were of technical grade and purchased from Honeywell. Reactions were monitored for completion by analysing a small sample by TLC. Thin layer chromatography (TLC): Merck TLC plates silica gel 60 on aluminium with the indicated solvent system; the spots were visualized by UV light (254 nm and 366 nm). UV-Vis spectra: Specord® 250 PLUS spectrophotometer (Analytic Jena, Germany); λ in nm. IR spectra: SpectrumTwo FT-IR Spectrometer (Perkin-Elmer, USA) equipped with a Specac Golden Gate™ ATR (attenuated total reflection) accessory; applied as neat samples; $1/\lambda$ in cm^{-1} . ¹H-NMR spectra in the indicated solvent; Bruker AV-400 (400 MHz); δ in ppm rel. to TMS (δ 0.00), J in Hz. ¹³C-NMR spectra in the indicated solvent; Bruker AV-500 (125.7 MHz); δ in ppm rel. to TMS (δ 0.0). ¹⁹⁵Pt-NMR spectra in the indicated solvent; Bruker AV-500 (107.5 MHz); δ in ppm rel. to K₂PtCl₆ in D₂O (δ 0). EI mass spectrometry was performed on a DFS double-focusing (BE geometry) magnetic sector mass spectrometer DFS (ThermoFisher Scientific, USA). Mass spectra were measured with electron ionization (EI) at 70 eV, solid probe inlet, source temperature of 200°C, acceleration voltage of 5 kV, and resolution of 2'500. The instrument was scanned between m/z 30 and 900 at scan rate of 2 s/decade in the magnetic scan mode. Perfluorokerosene (PFK, Fluorochem) served for calibration. ESI mass spectra were recorded on a Bruker maXis mass spectrometer. Samples were dissolved in an appropriate solvent at a concentration of around 1 $\mu\text{mol/mL}$ and measured at continuous flow at 3 $\mu\text{L/min}$. The mass spectrometer was operated in the positive electrospray ionization mode at 4'000 V capillary voltage, -500 V endplate offset, with a N₂ nebulizer pressure of 0.8 bar and dry gas flow of 4 L/min at 180°C. MS acquisitions were performed in the mass range from m/z 50 to 2'000 at 20'000 resolution (full width at half maximum) and 1.0 Hz spectra rate. Masses were calibrated between m/z 158 and 1450 or 2721 prior analysis below 2 ppm accuracy, with a 2 mM solution of sodium formate or with a Fluka electrospray calibration solution (Sigma-Aldrich) that has been 100 times diluted with acetonitrile, respectively. Elemental analysis was performed on a LECO Truespec CHNS(O)-microanalyser. The elemental analysis of the platinated species was done at the Mikrolabor of the Laboratorium für Organische Chemie at the ETHZ.

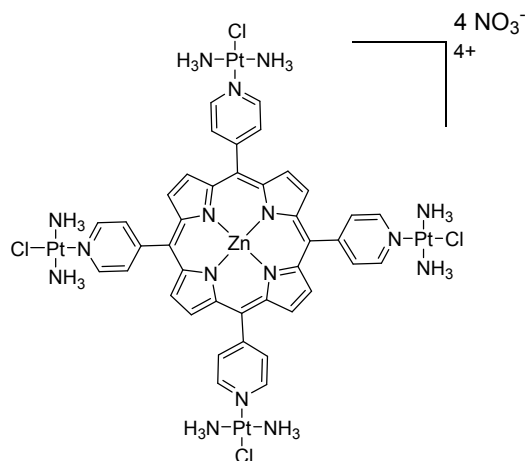
Synthetic procedures to yield platinated porphyrins **tPt-Zn4PyP**, **tPt-⁶⁷Zn4PyP**, **tPt-Cu4PyP**, **cPt-Zn4PyP**, **cPt-Cu4PyP**, **dPt-Zn4PyP**, **dPt-Cu4PyP** and *trans*-[Pt(NH₃)₂(pyridine)Cl]NO₃ (**tPt-Py**)

5,10,15,20-tetra(4'-pyridyl)-zinc(II)-porphyrin (**Zn4PyP**)¹



To a solution of **H₂4PyP** (0.032 mmol, 20.0 mg) in DMF:water (1:1, 3.0 mL) Zn(OAc)₂·2 H₂O (0.081 mmol, 18.0 mg) was slowly added. The solution was refluxed for 60 min (completion of reaction was monitored by HPLC) and then cooled to room temperature. Water was added to the solution to precipitate the product, which was further filtered and washed thoroughly with water, methanol and ether. The resulting violet solid product was obtained in 18.0 mg, 82 % yield. IR (KBr, cm⁻¹): 1604, 1594, 1409, 1338, 1205, 1072, 992, 790, 669; MS (ESI): *m/z* = 681 [M + H]⁺

[*trans*-PtCl(NH₃)₂]₄-5,10,15,20-tetra(4'-pyridyl)-zinc(II)porphyrin nitrate (**tPt-Zn4PyP**)



Transplatin (0.117 mmol, 35.3 mg) and silver nitrate (0.117 mmol, 19.9 mg) were dissolved in 2.0 mL of DMF and stirred in the dark at room temperature for 24 h. The resulted turbid solution was centrifuged to remove the white silver chloride. The light yellow colored solution was added to suspension of **Zn4PyP** (0.029 mmol, 20.1 mg) in 2.0 mL DMF and stirred in the dark at 50°C for 24 h. After that, the mixture was precipitated with diethyl ether. The solid was filtered and further washed with methanol, dichloromethane and diethyl ether. The solid was further dried in vacuum and the product was obtained in 51.0 mg, 87 % yield. IR (KBr, cm⁻¹): 3186, 3107, 1614, 1313, 994, 800, 720, 662; ¹H NMR (400 MHz; DMF-d₇): δ 9.42 (d, 8H, *J* = 6.4 Hz), 9.06 (s, 8H), 8.50 (d, 8H, *J* = 6.5 Hz), 4.79 (s, 24H); ¹⁹⁵Pt

NMR (107 MHz; DMF-d₇): δ -2309; MS (ESI): $m/z = 1272 [M - 3(\text{NO}_3) - 2\{\text{PtCl}(\text{NH}_3)_2\}]^+$, 945 $[M - 4(\text{NO}_3) - 3\{\text{PtCl}(\text{NH}_3)_2\}]^+$, 892 $[M - 4(\text{NO}_3) - 3\{\text{PtCl}(\text{NH}_3)_2\} - \text{Cl} - \text{NH}_3]^+$, 873 $[M - 4(\text{NO}_3) - 3\{\text{PtCl}(\text{NH}_3)_2\} - \text{Cl} - 2(\text{NH}_3)]^+$, 605 $[M - 4(\text{NO}_3) - 2\{\text{PtCl}(\text{NH}_3)_2\}]^{2+}$; Elemental analysis calcd (%) for C₄₀H₄₈Cl₄N₂₀O₁₂Pt₄Zn·2(H₂O): C 23.73, H 2.59, N 13.84; found: C 23.34, H 2.40, N 13.52.

Crystal structure determination of the cationic [*trans*-PtCl(NH₃)₂]₄-5,10,15,20-tetra(4'-pyridyl)-zinc(II)porphyrin unit. A saturated solution of **tPt-Zn4PyP** in DMF (about 1 mg in 0.5 mL of DMF) was subjected to the under oil crystallization following the procedure recently described by us². In short, 3.35 μL of the **tPt-Zn4PyP** DMF solution and 3.5 μL of each of the 96 aqueous solutions of the Small Molecule Anion screen³ were pipetted in 100 μL of silicone oil by a Crystal Gryphon LCP pipetting robot with a custom made Hamilton syringe holder. After one day, needle shaped crystals appeared in the drop originating from a 0.2 M aqueous solution of sodium tetraphenyl borate. Repeating the same procedure with **tPt-Zn4PyP** dissolved in water did not yield any crystals, most likely due to the too solubility of **tPt-Zn4PyP** in water. Crystallographic data were collected at 160.0(1) K on a Rigaku OD XtaLAB Synergy Dualflex diffractometer equipped with a Pilatus 200 K detector and a PhotonJet Cu K α source ($\lambda = 1.54184 \text{ \AA}$). Suitable crystals were covered with oil (Infineum V8512, formerly known as Paratone N), placed on a nylon loop that is mounted in a CrystalCap MagneticTM (Hampton Research) and immediately transferred to the diffractometer. The program suite *CrysAlis^{Pro}* was used for data collection, numerical and empirical absorption correction as well as data reduction.⁴ The structure was solved with direct methods using *ShelxT*⁵ and was refined by full-matrix least-squares methods on F^2 with *SHELXL-2014*⁶ using the GUI *OLEX2* (Table S1).⁷ The asymmetric unit contains one half of the molecule. Therefore, the central zinc metal center and the coordinated dimethylformamide solvent molecules are disordered in a 1:1 ratio. Furthermore, two more DMF molecules were disordered in a ratio of 58:42 and 56:44 respectively and had to be treated with suitable restraints. Graphical output was produced with the help of the program *Mercury*.⁸ CCDC 1977523 contains the supplementary crystallographic data for this paper. These data can be obtained free of charge from The Cambridge Crystallographic Data Centre via www.ccdc.cam.ac.uk/structures.

⁶⁷Zinc(II) chloride dihydrate (⁶⁷ZnCl₂ · 2 H₂O)

⁶⁷Zn (100.0 mg, 1.494 mmol) was dissolved in 5.0 mL of an aqueous solution of 16 % HCl and the mixture was stirred at room temperature until the solid had totally dissolved (30 minutes). The mixture was dried *in vacuo* by warming up the system to 55°C. The product was obtained as a white solid in a yield of 81 %. Analytical Data: ⁶⁷ZnCl₂ · 2 H₂O, Mol. Wt.: 173.86 g/mol. MS (EI): $m/z = 136.87$ (100%), 138.86 (66.9%), 140.86 (8.7%).

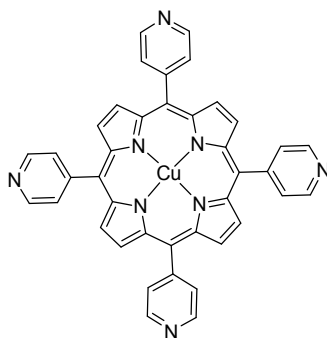
5,10,15,20-tetra(4'-pyridyl)-⁶⁷zinc(II)porphyrin (⁶⁷Zn4PyP)

The reaction of 5,10,15,20-tetra-(4'-pyridyl)-porphyrin with either zinc chloride or zinc acetate was optimized with respect to yield and minimal required excess of zinc. For these reactions, unlabelled zinc was used (Table S2). The best conditions applied with ⁶⁷Zn were as follows: 5,10,15,20-tetra-(4'-pyridyl)-porphyrin (40.0 mg, 0.051 mmol) was suspended in a mixture of 7.0 mL of DMF/water (1:1), then added to ⁶⁷ZnCl₂ · 2 H₂O (40.0 mg, 0.232 mmol). The mixture was stirred at 120°C for 26 h. After cooling down to room temperature, the product was precipitated with water, filtered and washed with water. The solid was taken up in a mixture of chloroform/methanol (3:2) and dried *in vacuo* to yield 34.0 mg of the porphyrin as a violet solid in a yield of 97%. Analytical Data: C₄₀H₂₄N₈⁶⁷Zn, Mol. Wt.: 683.62 g/mol. UV-Vis (DMF, λ; nm): 424.5 (Soret band), 404.9, 557.4, 596.3 (Q bands). MS (ESI): *m/z* = 684.14567 [M + H]⁺ (44%), 342.57721 [M + 2H]²⁺ (100%).

[*trans*-PtCl₂(NH₃)₂]₄-5,10,15,20-tetra(4'-pyridyl)-⁶⁷zinc(II)porphyrin nitrate (tPt-⁶⁷Zn4PyP)

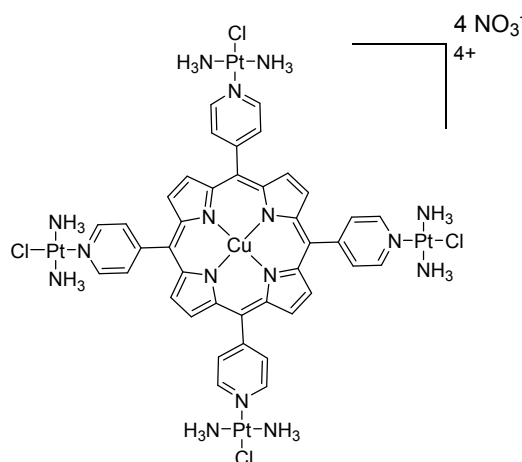
Transplatin (38.6 mg, 0.129 mmol) and silver nitrate (21.9 mg, 0.129 mmol) were dissolved in 2.0 mL DMF and stirred in the dark at room temperature for 24 h. The resulted suspension was centrifuged to remove the white silver chloride. The light yellow colored solution was added to a suspension of ⁶⁷Zn4PyP (20.0 mg, 0.029 mmol) in 2.0 mL DMF and stirred in the dark at 50°C for 48 h. The mixture was cooled down to room temperature, then 50% of the solvent was evaporated *in vacuo* and the porphyrin was subsequently precipitated with methyl *tert*-butyl ether. The precipitate was filtered and further washed with methanol, dichloromethane and methyl *tert*-butyl ether. Then, the solid was further dissolved in 2.0 mL DMF and centrifuged to remove insoluble impurities, before it was precipitated again with methyl *tert*-butyl ether. After having pipetted out the supernatant, the product was dried under vacuum and 28.5 mg of the product were obtained in 49% of yield as a violet solid. Analytical Data: C₄₀H₄₈Cl₄N₂₀O₁₂Pt₄⁶⁷Zn, Mol. Wt.: 1990.02 g/mol. ¹H-NMR (400 MHz, DMF-d₇): δ (ppm) 9.63 (d, *o*-pyridyl, 8 H, *J* = 4 Hz), 9.28 (β-pyrrole, s, 8H), 8.72-8.71 (*m*-pyridyl, d, 8 H, *J* = 4 Hz), 5.01 (NH₃, s, 24 H). ¹³C-NMR (125 MHz, DMF-d₇): δ (ppm) 153.37, 151.92, 149.09, 132.35, 132.06, 117.24. ¹⁹⁵Pt-NMR (107 MHz; DMF-d₇): δ (ppm) -2309. MS (ESI): *m/z* = 435.52079 [M]⁴⁺. Elemental analysis calcd. (%) for C₄₀H₄₈Cl₄N₂₀O₁₂Pt₄⁶⁷Zn·2(H₂O): C 23.71, H 2.59, N 13.83; found C 24.16, H 2.81, N 13.40.

5,10,15,20-tetra(4'-pyridyl)-copper(II)porphyrin (**Cu4PyP**)^{1b}



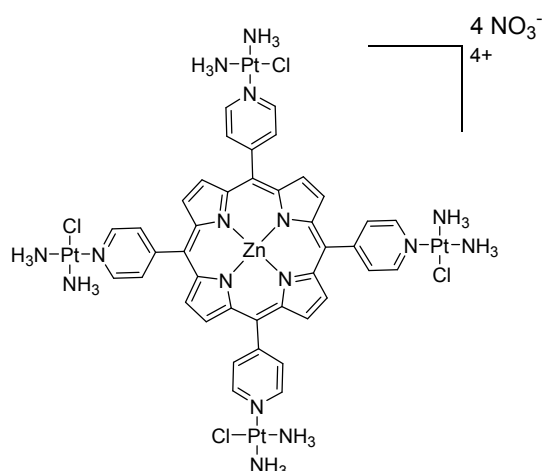
To a solution of **H₂4PyP** (0.032 mmol, 20.0 mg) in acetic acid (3.0 mL) Cu(OAc)₂·H₂O (0.202 mmol, 40.4 mg) dissolved in water (0.4 mL) was added. The solution was refluxed for 60 min (completion of reaction by monitored by HPLC) and then cooled to room temperature. Ammonia (25 %, 3.0 mL) was added to neutralize the solution and precipitate the product, which was further filtered and washed thoroughly with water, methanol and ether. The resulting violet solid product was obtained in 17.0 mg, 77 % yield. IR (KBr, cm⁻¹): 1590, 1404, 1347, 1002, 990, 798, 671; MS (ESI): *m/z* = 680 [M + H]⁺

[*trans*-PtCl(NH₃)₂]₄-5,10,15,20-tetra(4'-pyridyl)-copper(II)porphyrin nitrate (**tPt-Cu4PyP**)



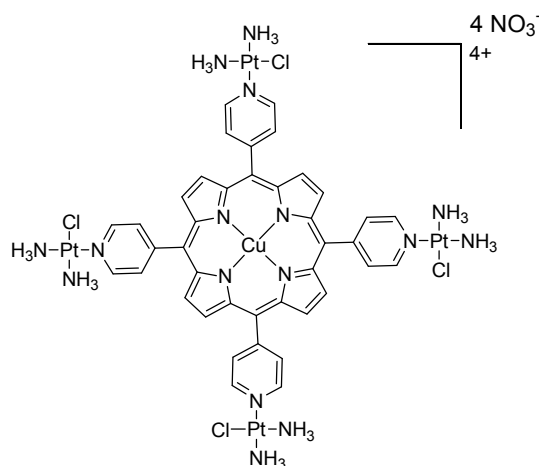
Transplatin (0.058 mmol, 17.7 mg) and silver nitrate (0.058 mmol, 9.9 mg) were dissolved in 1.0 mL of DMF and stirred at room temperature in the dark for 24 h. The resulted turbid solution was centrifuged to remove the white silver chloride. The light yellow colored solution was added to suspension of **Cu4PyP** (0.015 mmol, 9.9 mg) in 1.0 mL DMF and stirred at 50°C in the dark for 24 h. After that, the mixture was cooled down to room temperature and precipitated with diethyl ether. The solid was filtered and further washed with methanol, dichloromethane and diethyl ether. The solid was further dried in vacuum and the product was obtained in 23.0 mg, 79 % yield. IR (KBr, cm⁻¹): 3183, 3105, 1617, 1320, 999, 803, 721, 659; MS (ESI): *m/z* = 1271 [M - 3(NO₃) - 2{PtCl(NH₃)₂}]⁺, 944 [M - 4(NO₃) - 3{PtCl(NH₃)₂}]⁺, 891 [M - 4(NO₃) - 3{PtCl(NH₃)₂} - Cl - NH₃]⁺, 604 [M - 4(NO₃) - 2{PtCl(NH₃)₂}]²⁺; Elemental analysis calcd (%) for C₄₀H₄₈Cl₄N₂₀O₁₂Pt₄Cu: C 24.18, H 2.44, N 14.10; found: C 24.39, H 2.48, N 14.12.

[*cis*-PtCl(NH₃)₂]₄-5,10,15,20-tetra(4'-pyridyl)-zinc(II)porphyrin nitrate (**cPt-Zn4PyP**)



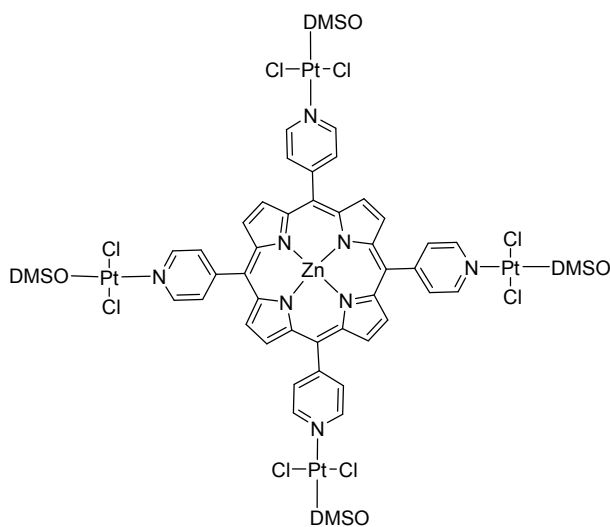
Cisplatin (0.029 mmol, 8.8 mg) and silver nitrate (0.029 mmol, 5.0 mg) were dissolved in 0.5 mL of DMF and stirred at room temperature in the dark for 24 h. The resulted turbid solution was centrifuged to remove the white silver chloride. The light yellow colored solution was added to suspension of **Zn4PyP** (0.007 mmol, 5.0 mg) in 0.5 mL DMF and stirred at 50°C in the dark for 24 h. After that, the mixture was cooled down to room temperature and precipitated with diethyl ether. The solid was filtered and further washed with methanol, dichloromethane and diethylether. The solid was further dried in vacuum and the product was obtained in 12.0 mg, 82 % yield. IR (KBr, cm⁻¹): 3202, 3111, 1614, 1312, 994, 795, 718, 662; ¹H NMR (500 MHz; DMF-d₇): δ 9.32 (d, 8H, *J* = 4.7 Hz), 9.01 (s, 8H), 8.48 (d, 8H, *J* = 4.2 Hz), 5.29 (s, 12H), 4.73 (s, 12H); ¹⁹⁵Pt NMR (107 MHz; DMF-d₇): δ -2292.6; MS (ESI): *m/z* = 1510.3 [M - 4(NO₃) - {PtCl(NH₃)₂} + Cl]⁺, 1228.6 [M - 4(NO₃) - 2{PtCl(NH₃)₂} - NH₃ + Cl]⁺, 910 [M - 4(NO₃) - 3{PtCl(NH₃)₂} - Cl]⁺; Elemental analysis calcd (%) for C₄₀H₄₈Cl₄N₂₀O₁₂Pt₄Zn·(MeOH)·(DMF): C 25.24, H 2.84, N 14.05; found: C 25.26, H 2.60, N 13.77.

$[cis\text{-PtCl}(\text{NH}_3)_2]_4\text{-5,10,15,20-tetra(4'-pyridyl)-copper(II)porphyrin nitrate (cPt-Cu4PyP)}$



Cisplatin (0.029 mmol, 8.8 mg) and silver nitrate (0.029 mmol, 5.0 mg) were dissolved in 0.5 mL of DMF and stirred in the dark at room temperature for 24 h. The resulted turbid solution was centrifuged to remove the white silver chloride. The light yellow colored solution was added to suspension of **Cu4PyP** (0.0074 mmol, 5.0 mg) in 0.5 mL DMF and stirred in the dark at 50°C for 24 h. After that, the mixture was cooled down to room temperature and precipitated with diethyl ether. The solid was filtered and further washed with methanol, dichloromethane and diethyl ether. The solid was further dried in vacuum and the product was obtained in 11.0 mg, 74 % yield. IR (KBr, cm^{-1}): 3190, 3107, 1614, 1305, 999, 797, 716, 660; MS (ESI): $m/z = 1509.3 [M - 4(\text{NO}_3) - \{\text{PtCl}(\text{NH}_3)_2\} + \text{Cl}]^+$, 1226.6 $[M - 4(\text{NO}_3) - 2\{\text{PtCl}(\text{NH}_3)_2\} - \text{NH}_3 + \text{Cl}]^+$, 909 $[M - 4(\text{NO}_3) - 3\{\text{PtCl}(\text{NH}_3)_2\} - \text{Cl}]^+$; Elemental analysis calcd (%) for $\text{C}_{40}\text{H}_{48}\text{Cl}_4\text{N}_{20}\text{O}_{12}\text{Pt}_4\text{Cu} \cdot (\text{MeOH})_{0.4} \cdot (\text{H}_2\text{O})_{1.5}$: C 23.94, H 2.62, N 13.82; found: C 23.99, H 2.29, N 13.51.

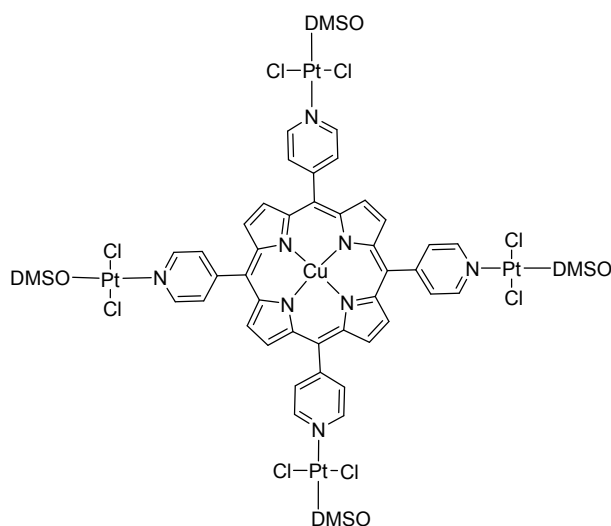
$[trans\text{-PtCl}_2(\text{DMSO})_2]_4\text{-5,10,15,20-tetra(4'-pyridyl)-zinc(II)porphyrin (dPt-Zn4PyP)}$



$cis\text{-Pt}(\text{DMSO})_2\text{Cl}_2$ (0.058 mmol, 24.7 mg) and **Zn4PyP** (0.015 mmol, 10.0 mg) were dissolved in 5.0 mL of dichloromethane and stirred in the dark for 4 h at 50°C. The reaction mixture was centrifuged

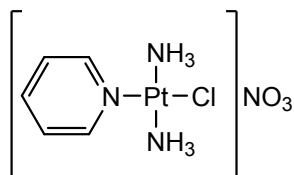
and solvent was removed. Subsequently 2.0 mL of dichloromethane were added before the mixture was centrifuged and the solvent was removed again (to remove unreacted *cis*-Pt(DMSO)₂Cl₂). The remaining solvent was removed *in vacuo*. The solid was further dried and the product was obtained in 27.0 mg, 89 % yield. IR (KBr, cm⁻¹): 1611, 1418, 1145, 1017, 995, 791, 695; ¹H NMR (400 MHz; DMF-d₇): δ 9.25 (dd, 8H, *J* = 5.2, 1.2 Hz), 9.04 (s, 8H), 8.62 (d, 8H, *J* = 5.2, 1.4 Hz), 3.65 (s, 24H); ¹⁹⁵Pt NMR (107 MHz; DMF-d₇): δ -3050; MS (ESI): *m/z* = 2094.5 [M + K]⁺, 2080.6 [M + Na]⁺, 1752 [M – Pt – DMSO – 2Cl + K]⁺, 1736 [M – Pt – DMSO – 2Cl + Na]⁺, 1408 [M – 2Pt – 2DMSO – 4Cl + K]⁺, 1392 [M – 2Pt – 2(DMSO) – 4Cl + Na]⁺, 1064 [M – 3 Pt – 4(DMSO) – 6Cl + K]⁺; Elemental analysis calcd (%) for C₄₈H₄₈Cl₈N₈O₄Pt₄S₄Zn: C 28.01, H 2.35, N 5.44; found: C 27.77, H 2.33, N 5.29.

[*trans*-PtCl(DMSO)₂]₄-5,10,15,20-tetra(4'-pyridyl)-copper(II)porphyrin (**dPt-Cu4PyP**)



cis-Pt(DMSO)₂Cl₂ (0.064 mmol, 27.3 mg) and **Cu4PyP** (0.016 mmol, 11.0 mg) were dissolved in 5.0 mL of dichloromethane and stirred in the dark for 4 h at 50°C. The reaction mixture was centrifuged and solvent was removed. Subsequently 2.0 mL of dichloromethane were added before the mixture was centrifuged and the solvent was removed again (to remove unreacted *cis*-Pt(DMSO)₂Cl₂). The remaining solvent was removed *in vacuo*. The solid was further dried and the product was obtained in 32.0 mg, 92 % yield. IR (KBr, cm⁻¹): 1610, 1417, 1147, 1019, 999, 696; MS (ESI): *m/z* = 2015.7 [M-Cl]⁺, 1752 [M – Pt – DMSO – 2Cl + K]⁺, 1674.0 [M – Pt – 2(DMSO) – 2Cl + K]⁺, 1408 [M – 2 Pt – 2(DMSO) – 4Cl + K]⁺, 1330 [M – 2 Pt – 3(DMSO) – 4Cl + K]⁺, 1064 [M – 3Pt – 4(DMSO) – 6Cl + K]⁺; Elemental analysis calcd (%) for C₄₈H₄₈Cl₈N₈O₄Pt₄S₄Cu: C 28.03, H 2.35, N 5.45; found: C 27.95, H 2.31, N 5.37.

trans-[Pt(NH₃)₂(pyridine)Cl]NO₃ (**tPt-Py**)⁹



Transplatin (0.331 mmol, 100.0 mg) and silver nitrate (0.331 mmol, 56.0 mg) were dissolved in 5.0 mL of DMF and stirred in the dark at 50°C for 24 h. The resulted turbid solution was centrifuged to remove the white silver chloride. The light yellow colored solution was added to pyridine (24.0 μ L, 0.302 mmol) and stirred at 50°C in the dark for 24 h. After that, the mixture was cooled down to room temperature and the solvent was evaporated with the aid of a rotary evaporator. The residue was dissolved in 10 mL methanol and subsequently filtered. Diethyl ether was added to the filtrate, the formed precipitate was collected and washed with diethyl ether. The precipitate was dissolved again in methanol and added dropwise to vigorously stirred diethyl ether to obtain **tPt-Py** after collecting and drying in vacuum as a white solid in 65.0 mg, 49 % yield. IR (Golden-Gate, cm⁻¹): 3260, 3119, 1652, 1611, 1586, 1456, 1346, 1304, 1242, 1162, 1078, 1021, 944, 871, 824, 760, 687, 661. ¹H-NMR (400 MHz; DMF-d₇): 9.00 (*dd*, *J* = 6.6, 1.5 Hz, 2H, 2 x arom. N-CH); 8.15 (*t*, *J* = 7.7 Hz, 1H, 1 x arom. N-CH-CH-CH); 7.69 (*t*, *J* = 7.0 Hz, 2H, 2 x arom. N-CH-CH); 4.52 (broad. *s*, 6H, 2 x NH₃). ¹³C-NMR (125 MHz; DMF-d₇): 154.1 (*d*, 2 x arom. N-CH); 149.5 (*d*, 1 x arom. N-CH-CH-CH); 127.1 (*d*, 2 x arom. N-CH-CH). ¹⁹⁵Pt-NMR (107 MHz; DMF-d₇): -2306 (*s*, Pt). MS (ESI): *m/z* = 343 [M - NO₃]⁺. Elemental analysis calcd (%) for C₅H₁₁ClN₄O₃Pt: C 14.80, H 2.73, N 13.81; found: C 14.89, H 2.70, N 13.68.

Singlet oxygen quantum yields:

The singlet oxygen quantum yields (Φ_{Δ}) of **tPt-H₂4PyP**, **cPt-H₂4PyP**, **tPt-Zn4PyP** and **cPt-Zn4PyP** were determined analogously to a method reported by our group.¹⁰ The PSs were dissolved in D₂O and the solutions were placed in a glass cuvette (114F-10-40, 10 mm × 4 mm dimensions, Hellma Analytics, Germany). Two different concentrations were prepared for each PS, corresponding to maximum absorption intensities of approximately 1.0 and 0.5, with the cuvette oriented in a way that the light path equals to 10 mm. The cuvettes containing solutions of the same concentration as used for the corresponding UV-Vis spectroscopy were placed in a CUV-UV/VIS-TC-ABS temperature-controlled Qpod sample compartment (Avantes, The Netherlands) and cooled to 20°C; temperature control was performed with the use of a TC-125 controller (Quantum Northwest, USA) and Q-Blue software. Emission spectroscopy was conducted in a custom-built setup¹⁰, that is based on the setup described by Bonnet and co-workers.¹¹ Excitation was performed using a high-power-LED 420 nm light source (FC5-LED-WL, Prizmatix Ltd., Israel). The light source was connected with an optical fibre (1000 µm core diameter, Avantes) to the cuvette holder over a SMA 905 fibre optic connector. The intensity of the light source was measured to be 22.8 mW / cm² at the position of the cuvette. The excitation power was measured using a S310C thermal sensor connected to a PM100USB power meter (Thorlabs, Germany). The connection piece used to insert the SMA connector into the cuvette holder was replaced by an in-house custom-built connection piece that allows the fibre to be inserted at a distance of 2.0 cm from the cuvette. The detector (AvaSpec-NIR256-1.7TEC, Avantes) was set to 0°C and connected to the cuvette holder with an optical fibre (600 µm diameter, Avantes). Emission spectra were collected at a 90° angle with respect to the excitation beam from 1050 nm to 1500 nm after two measurement runs; every measurement run consisted of five averaged measurements each lasting 9 s. All spectra were recorded using AvaSoft 8.9 software from Avantes and further processed using Microsoft Office Excel and Origin 2018 software.

The singlet oxygen quantum yields were calculated by comparison with meso-tetrakis(4'-sulphonatophenyl)porphine tetraammonium (**TPPS**), according to equation E1. It was assumed that the singlet oxygen quantum yield of this compound is identical to the one of the analogous tetrasodium salt ($\Phi_{\Delta} = 0.62$ in H₂O¹²).

$$(E1) \quad \Phi_{\Delta(x)} = \Phi_{\Delta(std)} \left(\frac{I_{std}^{420}}{I_x^{420}} \right) \left(\frac{E_x}{E_{std}} \right)$$

In E1, the subscript “x” designates the corresponding photosensitizer and “std” the standard (**TPPS**), respectively. “ Φ_{Δ} ” is the singlet oxygen quantum yield. “ I^{420} ” is the rate of light absorption calculated as overlap of the absorption spectrum of either PS or standard and the emission spectrum of the LED light source at 420 nm (I_0). The absorption intensity depends exponentially on absorbance A (E2). For A, the measured absorbance values were scaled by a factor of 0.4. E is the integrated emission peak of

singlet oxygen at around 1270 nm. For these emission spectra, the integrated values were obtained by applying a manual background correction in Origin.

$$(E2) \quad I^{420} = I_0(1 - 10^{-A})$$

E1 can be rewritten as:

$$(E3) \quad \Phi_{\Delta(x)} = \Phi_{\Delta(std)} \left(\frac{S_x}{S_{std}} \right)$$

In E3, “S” designates the slope when “E” is plotted against “I⁴²⁰” for the two measured concentrations, with a fixed intercept at 0. Errors of the singlet oxygen quantum yields were calculated by error propagation from the standard errors of “S_x” and “S_{std}”.

Cell Culture:

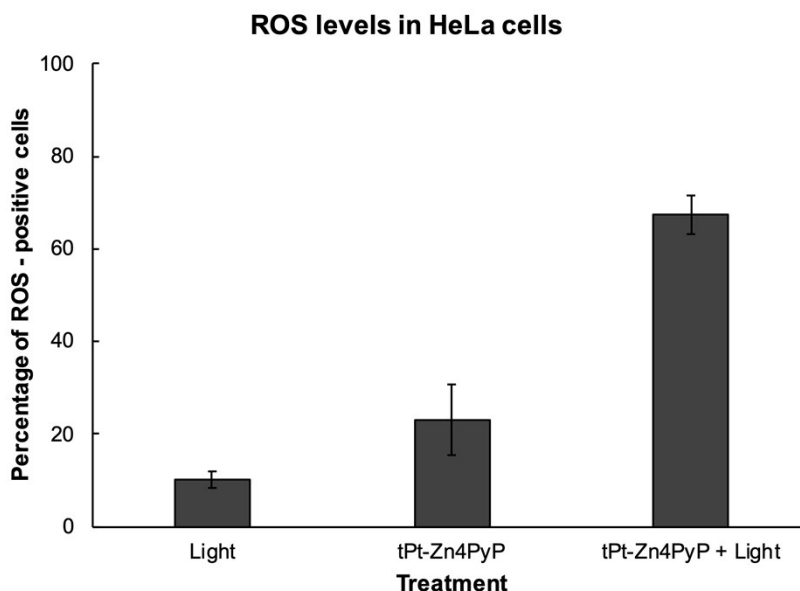
Human cervical carcinoma (HeLa) cells were cultured in DMEM (Gibco) supplemented with 5% fetal calf serum (FCS, Gibco), 100 U/mL penicillin, 100 µg/mL streptomycin. The normal human fetal lung fibroblast cell line (MRC-5) was grown in MEM medium (Gibco) supplemented with 10% FCS (Gibco), penicillin (100 U/mL), and streptomycin (100 µg/mL). The cells were cultured at 37 °C and in 6% CO₂ humidified atmosphere.

Cytotoxicity studies:

Cytotoxicity studies in the dark and after light irradiation of complexes **tPt-Zn4PyP**, **tPt-Cu4PyP**, **cPt-Zn4PyP**, **cPt-Cu4PyP**, **dPt-Zn4PyP**, **dPt-Cu4PyP** and *cis*Pt(DMSO)₂Cl₂ (**dPt**) were performed on the HeLa cervical cancer cell line and the MRC5 fibroblast non-tumorigenic cell line by a fluorometric cell viability assay using resazurin (PromoCell GmbH, Germany). Cells were grown in triplicates in 96-well plates at a density of 4 × 10³ cells/well in 100 µL. One day later, cells were treated with increasing concentrations of the metal porphyrin complexes for 4 h, following which the growth medium was replaced with fresh medium. The plates were irradiated for 15 min at 420 nm in a Rayonet Chamber Reactor Complex (6.95 J / cm²). Cells were further incubated for 44 h, the medium was removed, and 100 µL of growth medium containing resazurin (0.2 mg / mL final concentration) was added. After 4 h, the fluorescence of the resorufin product was quantified at 590 nm emission with 540 nm excitation wavelength in a SpectraMax M5 microplate Reader. The results are expressed as mean ± error bar of independent experiments (Table 1). A series of negative controls (with cells treated with the porphyrin metal complexes in the dark) and positive controls (the porphyrin ligand together with cisplatin (**cPt**) to evaluate their possible combined action) were also performed.

Detection of Intracellular ROS Levels

3×10^5 HeLa cells in 2 ml DMEM supplemented with 5% FBS were seeded on 60 mm dishes. The following day, cells were treated with 10 nM **tPt-Zn4PyP** for 4 hours. Following the incubation, cells were washed with PBS and the medium was subsequently replaced with 2 mL DMEM. Cells were irradiated with 420 nm light for 15 min. After irradiation, H₂DCF-DA was added to the samples to a final concentration of 50 μ M and incubated for 90 minutes at 37°C. Cells were washed twice with PBS and collected by trypsinisation. Cells were suspended in 1ml PBS containing 1% FBS. Samples were analysed on an Attune NxT Cytometer (Thermo Fisher Scientific) using BL1 channel (excitation 488 nm, emission 515 nm) to measure DCF fluorescence. Results are expressed as mean percentage of ROS-positive cells over total cell population, obtained from three independent experiments with a minimum of 100 000 cells analysed per condition. The error bars represent standard deviation (S.D).



Localization studies using laser scanning confocal microscopy:

HeLa cells were seeded in Ibidi μ -Slide 8-well glass bottom dishes. Upon ≈ 70 % confluence, the growth medium was replaced with medium containing freshly prepared solutions of drugs at a final concentration of 1 μ M. After 2 h incubation with compounds, cells were washed three times with PBS (0.5 mL) and stained with the GOLGI ID[®] Green assay kit (ENZ-51028, Enzo Life Sciences, Inc., Switzerland) according to the manufacturer's protocol. Prior to imaging, cells were incubated for 5 min with Hoechst 33258 (1.5 μ M final concentration). Finally, cells were kept in fresh media containing 10 % FBS for live-cell imaging. The fluorescence of the GOLGI-ID[®] Green dye was visualized using excitation at 488 nm and emission at 550-600 nm, the one of the photosensitizers using excitation at 514 nm and emission at 650-750 nm (using a longpass filter) and the one of Hoechst 33342 using excitation at 405 nm and emission at 450-500 nm.

Immunofluorescence:

Coverslips, sterilized by washing them with 70% EtOH and brief flaming, were placed in 60 mm cell culture dishes. Cells were grown on coverslips to attain 80% confluence and were incubated with the corresponding photosensitizer for 14 hours at 37°C. Next, the cells on the coverslips were washed three times with PBS in order to remove the non-uptaken PS. The control samples and samples were kept in the dark and were then directly fixed, while samples undergoing light irradiation were first exposed to light for 15 min at 420 nm (light dose 6.95 J / cm²). Cells were fixed for 5 minutes at room temperature with a freshly-prepared 4% (v/v) formaldehyde solution from a 37% stock solution diluted in PBS buffer. Coverslips were washed with PBS and permeabilized with 0.2% (v/v) Triton X-100 from a 25% stock solution diluted with PBS for 5 min at room temperature. Coverslips were washed twice with PBS and blocked for 20 minutes at room temperature in a 2% (w/v) BSA solution in PBS. The primary antibody (mouse anti- γ H2AX(S139), 1:800) was diluted in 2% (w/v) BSA in PBS solution. Antibody solution (35 μ L per coverslip) were pipetted per coverslip onto parafilm in a humidifying chamber. Coverslips were placed and incubated with the antibody mix over night at 4 °C, were washed the next day twice with PBS and incubated with the secondary antibody (goat anti-mouse Alexa fluor 594, 1:800) in the dark at 37°C for 1 h. After that, coverslips were washed twice with PBS and incubated with 1 μ g/mL DAPI in PBS for 10 min at room temperature in the dark. Finally, coverslips were washed twice with PBS and once with H₂O and mounted with 5 μ L Vectashield[®] mounting medium onto glass slides. The slides were left at 4°C for 1 h and then the edges were sealed with nail polish. Image acquisition was performed on CLSM - Leica SP8 inverse STED 3X maintained by the Center for Microscopy and Image Analysis, University of Zurich, and the images were analyzed using Fiji (version 2.0.0-rc-49/1.52i).

Sample Preparation for ICP-MS:

HeLa cells were seeded a week before treatment at a concentration of 1×10^6 cells / mL in a 15 cm² cell culture Petri dish, allowed to grow until 80% confluence and incubated in cell culture medium with the target compounds (previously dissolved in DMF as vehicle, v/v < 0.1%) at a concentration of 10.0 μ M for 4 h. The medium was removed, the cells washed with PBS and trypsinized. After re-suspension in PBS, the pellet was washed with ice cold PBS and collected per centrifugation at 600 g for 5 min at 4°C. The organelles were isolated via differential centrifugation. Briefly, the collected pellets were re-dissolved in 2.0 mL of extraction buffer containing protease inhibitor cocktail (Cat. Nr: LYSIS01, Sigma-Aldrich, Switzerland) and incubated for 15 min on ice. The samples were then homogenized with a pre-chilled Dounce homogenizer (7 mL, tight pestle A, ~25 strokes) and centrifuged at 1000 g for 10 min at 4°C. After centrifugation, the pellet obtained was re-dissolved in 2 mL of a sucrose solution (0.25 M sucrose, 10 mM MgCl₂) and layered with 2 mL of a second hypertonic sucrose solution (0.55 M sucrose, 0.5 mM MgCl₂). The suspension was centrifuged twice at 1450 g and 4°C for 5 min. The pellet was re-suspended in 3 mL of the second sucrose solution and centrifuged at 1450 g and 4°C for 5 min to obtain the nuclear extract. These steps of the isolation procedure were monitored under phase contrast microscope on Menzel-Gläser coverslips (Olympus IX81 microscope).¹³ The supernatant phases removed during the isolation of nuclei were collected and formed the “residual” fraction. An aliquot of crude lysate after homogenization, nuclear and residual fraction was each used for protein quantification using the Bradford method.¹⁴ The isolated samples were then lyophilized on an Alpha 2-4 LD plus (CHRIST, Germany). The resulting samples underwent chemical digestion with 10 mL of a 2% nitrohydrochloric acid solution for 24 h. The resulting suspensions were filtered on 0.20 μ m non-pyrogenic sterile Filtropur filters (Sarstedt, Switzerland) and the obtained samples were injected in ICP-MS.

ICP-MS Studies:

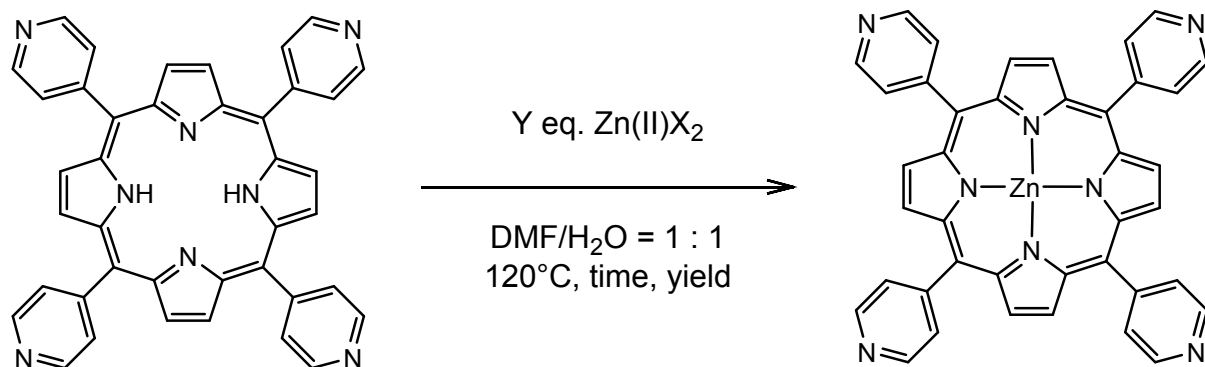
ICP-MS measurements were performed on an Agilent QQQ 8800 Triple quad ICP-MS spectrometer (Agilent Technologies, Switzerland) with an ASX200 autosampler (Agilent Technologies, Switzerland), equipped with standard nickel cones and a “micro-mist” quartz nebulizer fed with 0.3 mL/min analytic flow (as a 2 % HNO₃ aqueous solution). Platinum and zinc were measured against a platinum and zinc single element standard (Merck 1703410100 and Merck 1703890100, respectively) and verified by a control (Agilent 5188-6524 PA Tuning 2). Metals content of the samples was determined by means of a 9-step serial dilution in the range between 0 and 500 ppb in metals (R>0.99) with a background equivalent concentration of BEC: 8.4 ppt and a detection limit of DL: 20 ppt. The isotopes ¹⁹⁴Pt (32.97 % abundance), ¹⁹⁵Pt (33.83% abundance) and ⁶⁷Zn (4.1% abundance) were evaluated in “no-gas” mode and He-gas mode. Spiking the samples with untreated negative controls (to account for eventual carbon content from the biological samples) resulted in equivalent values within error ranges. A solution of indium (500 ppb) and tungsten (500 ppb) was used as internal standard. The results are expressed as ng

metals / mg protein (correction due to the different mass of the observed cellular compartments), as mean \pm standard deviation error of different independent experiments.

Table S1: Crystal data of [*trans*-PtCl(NH₃)₂]₄-5,10,15,20-tetra(4'-pyridyl)-zinc(II)porphyrin tetraphenylborate · 7 DMF

Empirical formula	C ₁₆₀ H ₁₈₄ B ₄ Cl ₄ N ₂₄ O ₈ Pt ₄ Zn
Formula weight	3602.07
Crystal system	Triclinic
Space group	P-1
a [Å]	12.1513(2)
b [Å]	17.9898(2)
c [Å]	19.21888(13)
α [°]	77.5748(8)
β [°]	80.9900(10)
γ [°]	89.3233(12)
Volume [Å ³]	4051.16(9)
Z	1
Density (calculated) [Mg/m ³]	1.476
Temperature [K]	160.00(10)
Wavelength [Å]	1.54184
Absorption coefficient [mm ⁻¹]	7.556
F(000)	1806
Crystal size [mm ³]	0.321 x 0.034 x 0.03
Crystal description	red needle
Theta range for data collection [°]	3.684 to 80.096
Index ranges	-15 \leq h \leq 15, -22 \leq k \leq 22, -23 \leq l \leq 24
Reflections collected	144826
Independent reflections	17213 [R(int) = 0.0697]
Reflections observed	15220
Criterion for observation	I > 2 σ (I)
Completeness to theta	99.9 % to 67.684°
Absorption correction	Gaussian
Max. and min. transmission	1.000 and 0.204
Data / restraints / parameters	17213 / 104 / 950
Goodness-of-fit on F ²	1.037
Final R indices [I > 2 σ (I)]	R1 = 0.0684, wR2 = 0.1917
R indices (all data)	R1 = 0.0736, wR2 = 0.1964
Largest diff. peak and hole [e.Å ⁻³]	6.611 and -2.481

Table S2: Optimisation of the zinc(II) insertion into **H₂4PyP**



Zinc(II) salt	Equivalents of Zn(II)	Time	Yield
Zn(OAc) ₂ ·2 H ₂ O	6	48 h	88 %
ZnCl ₂ ·2 H ₂ O	6	26 h	96 %
ZnCl ₂ ·2 H ₂ O	5	26 h	87 %
ZnCl ₂ ·2 H ₂ O	4	26 h	90 %

The reactions were monitored by UV-Vis spectroscopy and ¹H-NMR.

Table S3: Singlet oxygen quantum yields (Φ_{Δ}) of **tPt-H₂4PyP**, **cPt-H₂4PyP**, **tPt-Zn4PyP** and **cPt-Zn4PyP** determined by the direct method in D₂O with irradiation at 420 nm (TPPS as standard ¹²).

	Φ_{Δ} (D ₂ O)
tPt-H₂4PyP	0.65 ± 0.04
tPt-Zn4PyP	0.74 ± 0.03
cPt-H₂4PyP	0.65 ± 0.06
cPt-Zn4PyP	0.47 ± 0.02
dPt-H₂4PyP	n.d. (insoluble)
dPt-Zn4PyP	n.d. (insoluble)

n.d. = not determined

Table S4: Pt and ⁶⁷Zn content in the different cellular compartments of HeLa cells treated for 4 h at 10 μM with complex **tPt-⁶⁷Zn4PyP**; results are expressed in a) nmol metal / mg protein and b) in ng metal / mg protein.

a)

	Nucleus	Non-nucleus
⁶⁷Zn	11.9 ± 4.4	11 ± 2.8
Pt	3.8 ± 1.0	4.7 ± 1.7

b)

	Nucleus	Residual	Total
⁶⁷Zn	795 ± 298	763 ± 190	1558 ± 23
Pt	745 ± 200	926 ± 326	1671 ± 345

Fig. S1: Reaction mechanism of the platination of a guanine nucleobase by platinated porphyrins

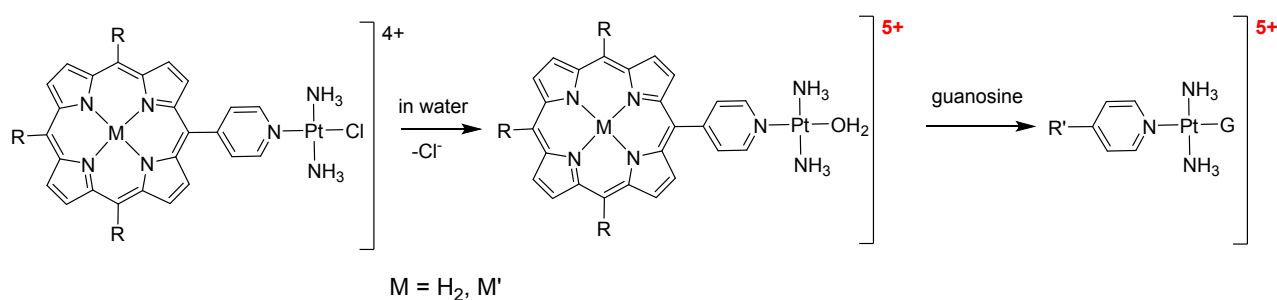
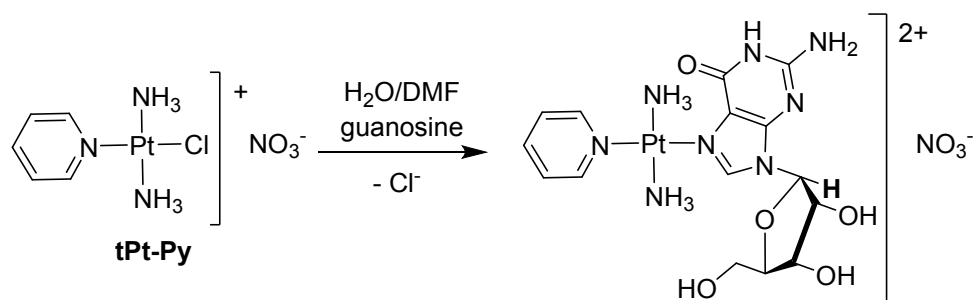


Fig. S2: Reaction of *trans*-[Pt(NH₃)₂(pyridine)Cl]NO₃ (**tPt-Py**) with guanosine.



NMR study to determine the reaction kinetics of **tPt-Py** and one equivalent of guanosine

The reaction of **tPt-Py** and one equivalent of guanosine was monitored by ¹H-NMR spectroscopy in a 1:1 DMF-d₇:D₂O mixture with a substance concentration of 618 μM. The spectra were recorded at intervals of 2.5 h, and 65 spectra were recorded in total. In the ¹H-NMR spectrum of the free guanosine, the H8 and H1' resonances are located at 8.11 and 5.95 ppm, respectively.¹⁵ Binding of **tPt-Py** that has lost its chloride ion results in a downfield shift for the two signals: for H8 the new signal is located at 8.95 ppm and for H1' the new signal (highlighted in bold in Figure S2) is located at 6.13 ppm. The recorded spectra are shown in Figure S3. The integrals of the signal at 5.95 ppm and the signals at 6.13 ppm are equal in the 27th spectrum recorded, showing that 50% of the binding occurred after nearly three days.

Since guanosine and **tPt-Py** react with a 1:1 stoichiometry, the assumption was made that the reaction can be treated as a second order reaction. For second order reactions, the inverse of the concentration vs. time plots results in a straight line, where the slope *S* is equal to *k*, the reaction rate constant. This was applied to the signal at 5.95 ppm, where the decay was plotted as the inverse of the concentration vs. time (Figure S4). The values of the first six spectra were not considered due to a high background. The plotted values result in a straight line, showing that the reaction was a second order reaction. The determined slope *S* is equal to a second order reaction constant *k* of 0.0034 M⁻¹s⁻¹ ± 0.0001 M⁻¹s⁻¹.

Fig. S3: Overview
guanosin

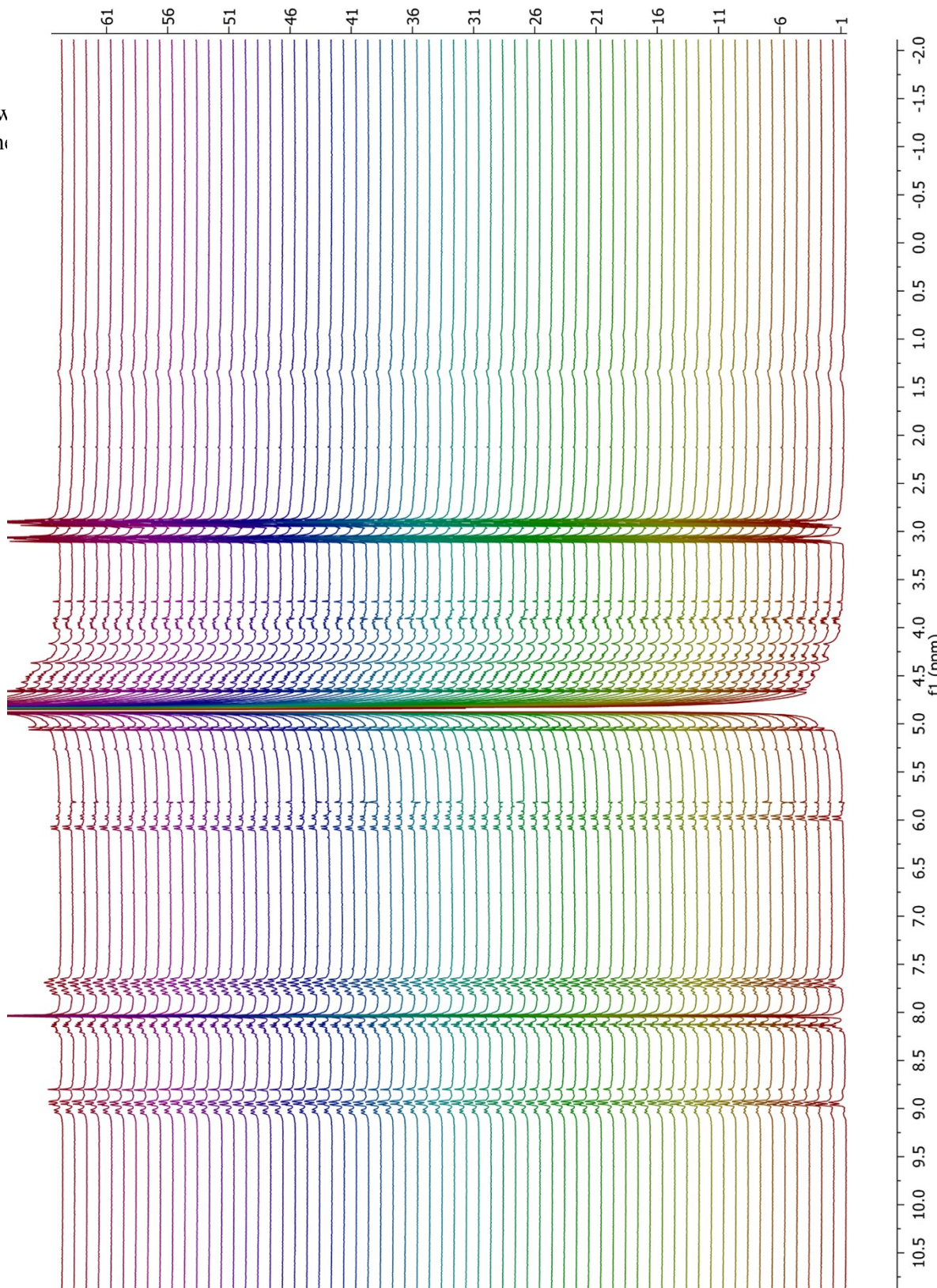


Fig. S4: Inverse of the concentration vs. time plot for the signal at 5.95 ppm of the reaction of **tPt-Py** with guanosine in a 1:1 DMF-d₇:D₂O mixture

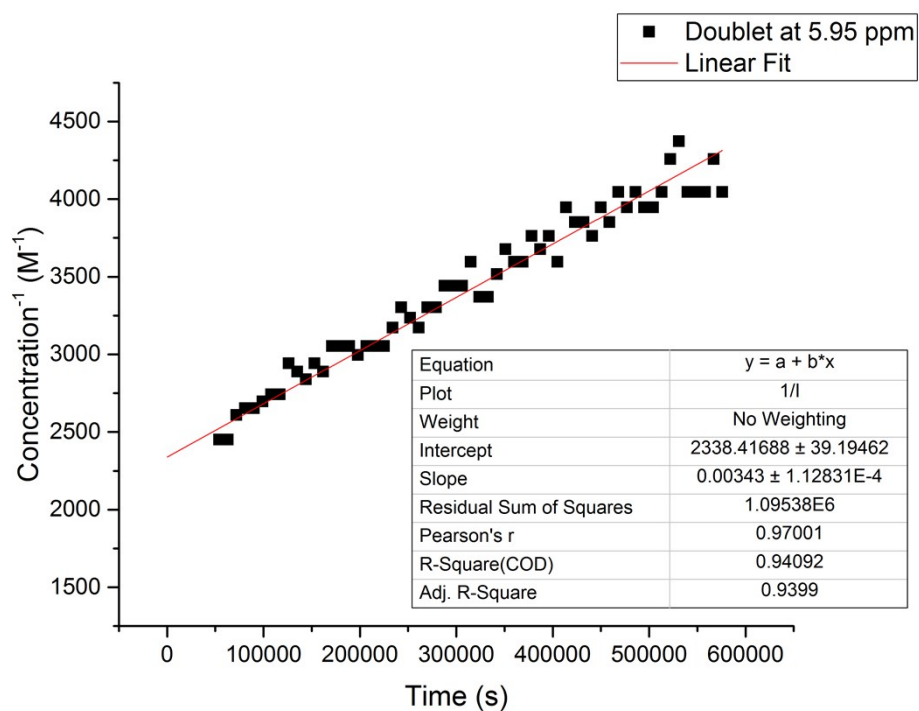


Fig. S5: HR-ESI-MS of $^{67}\text{Zn4PyP}$

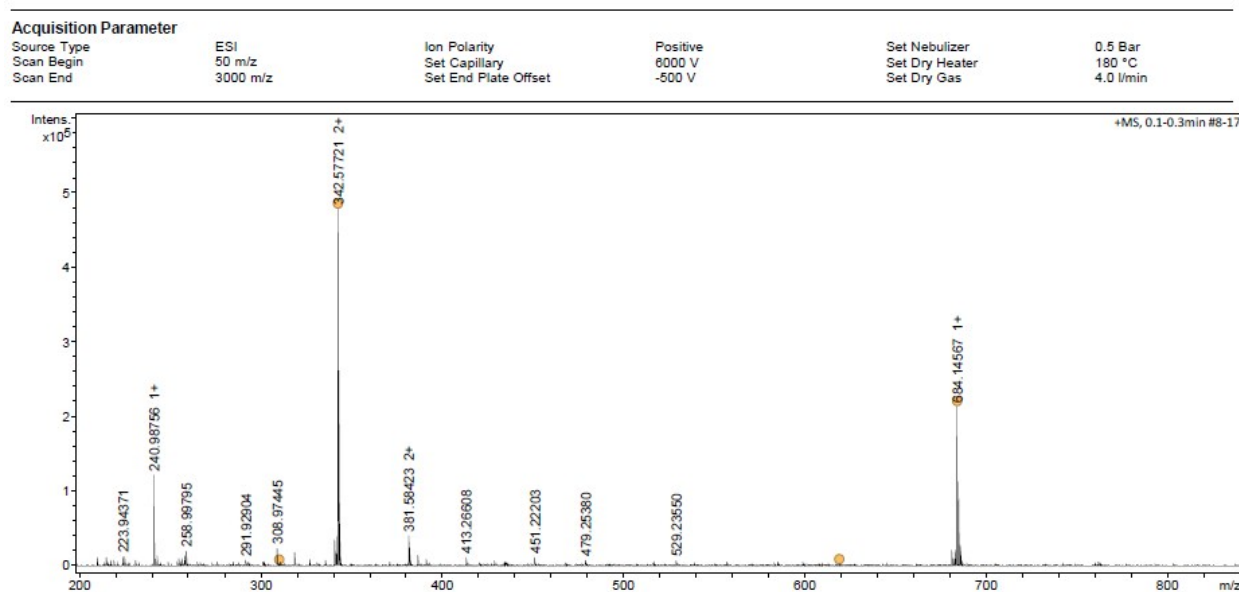


Fig. S6: UV-Vis of $^{67}\text{Zn4PyP}$ in DMF

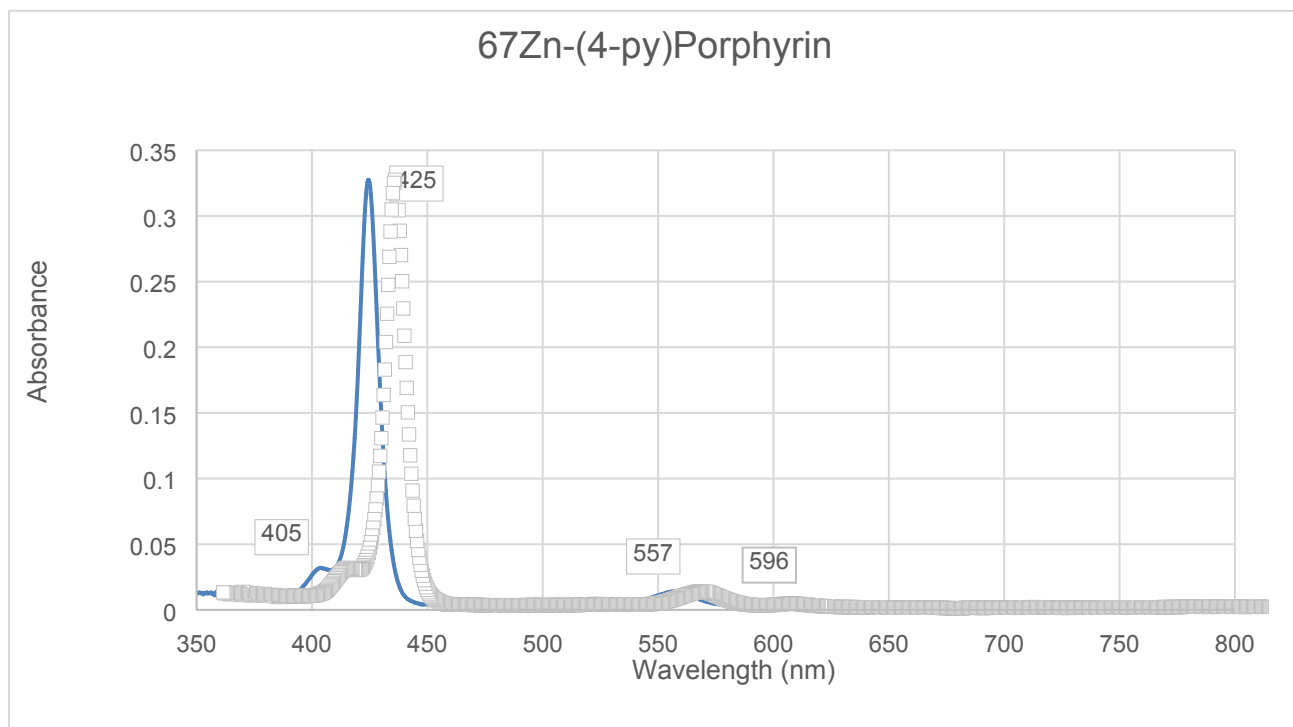


Fig. S7: HR-ESI-MS of **tPt-⁶⁷Zn4PyP**

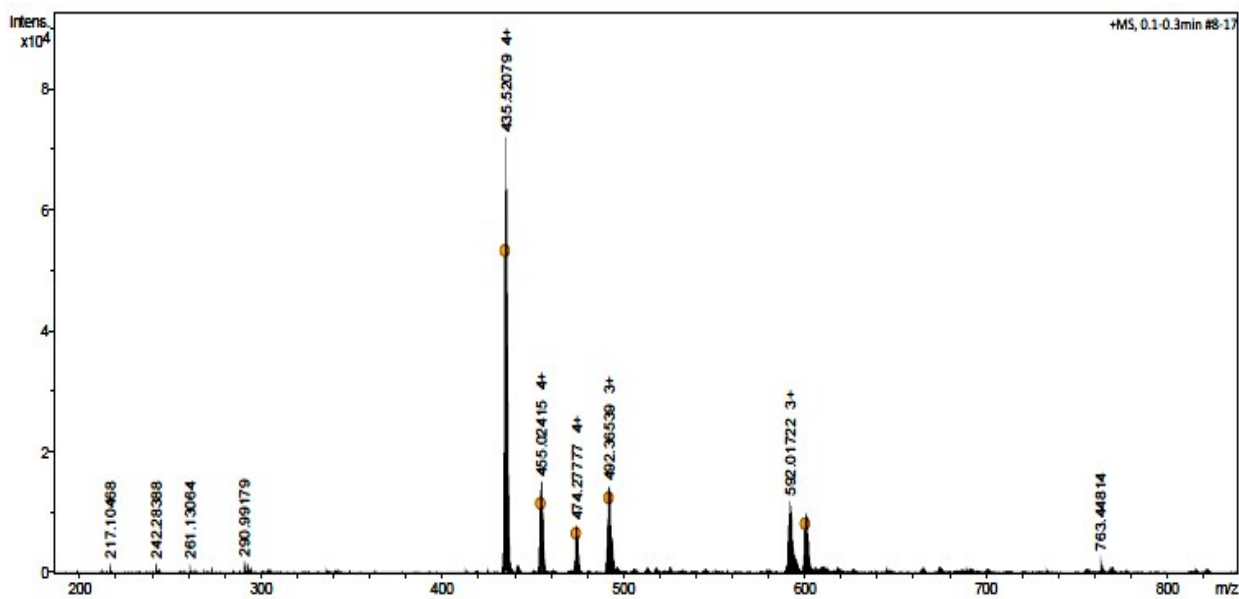


Fig. S8: ¹H-NMR of **tPt-⁶⁷Zn4PyP** in DMF-d₇

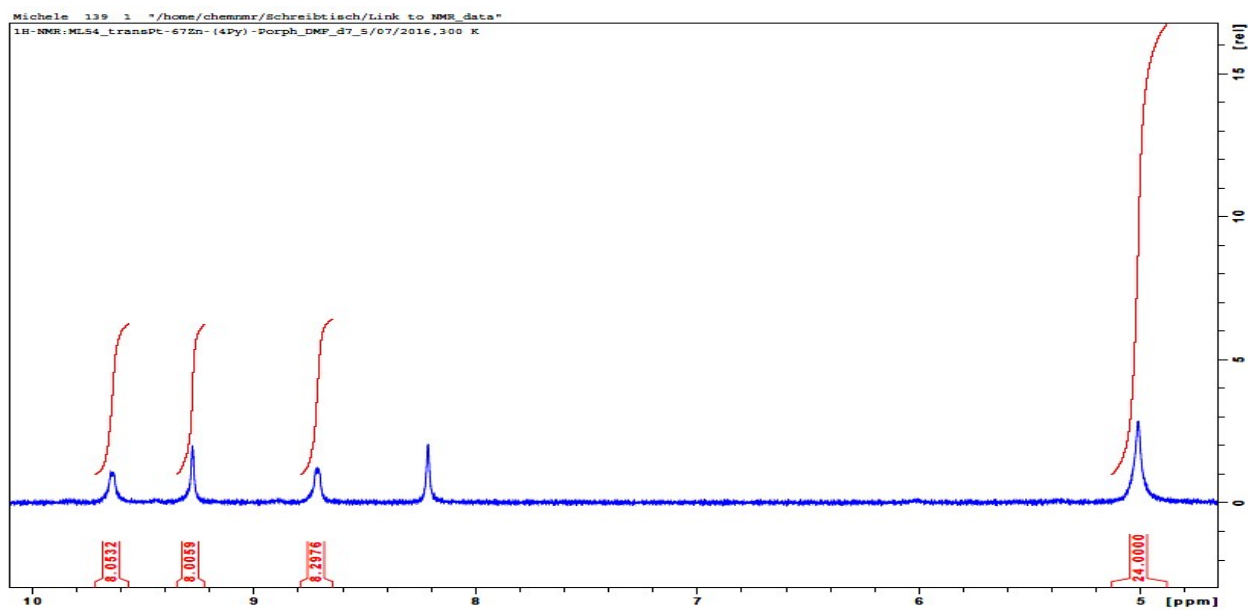


Fig. S9: ^{13}C -NMR of $\text{tPt-}^{67}\text{Zn4PyP}$ in DMF-d_7

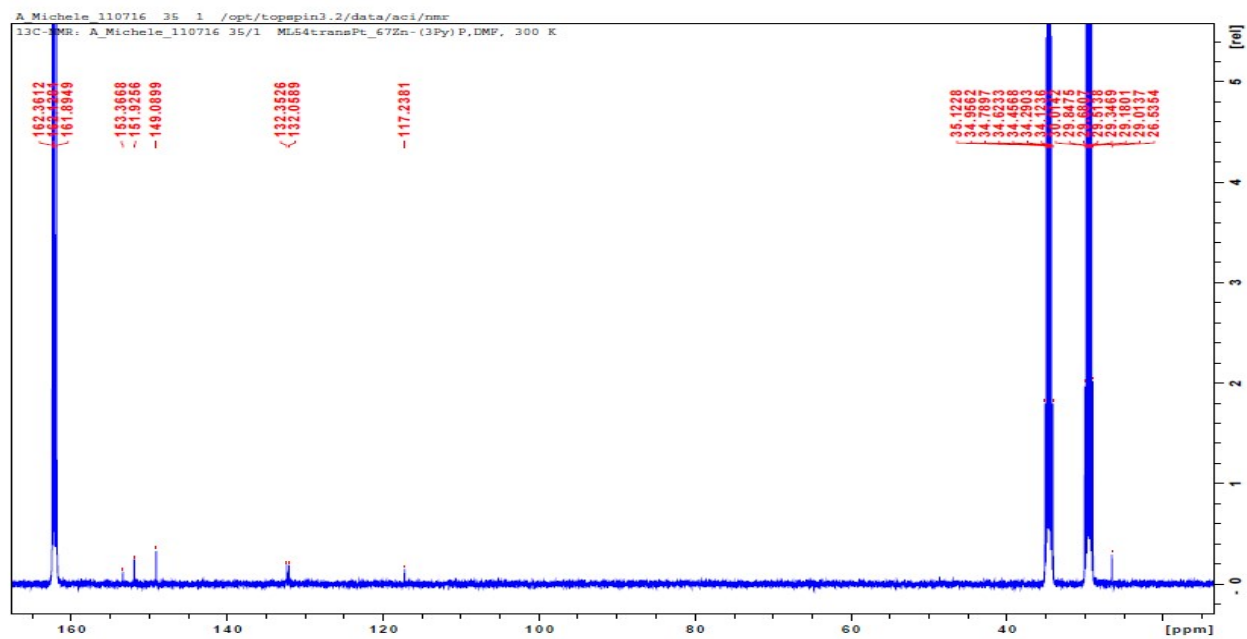


Fig. S10: ^{195}Pt -NMR of $\text{tPt-}^{67}\text{Zn4PyP}$ in DMF-d_7

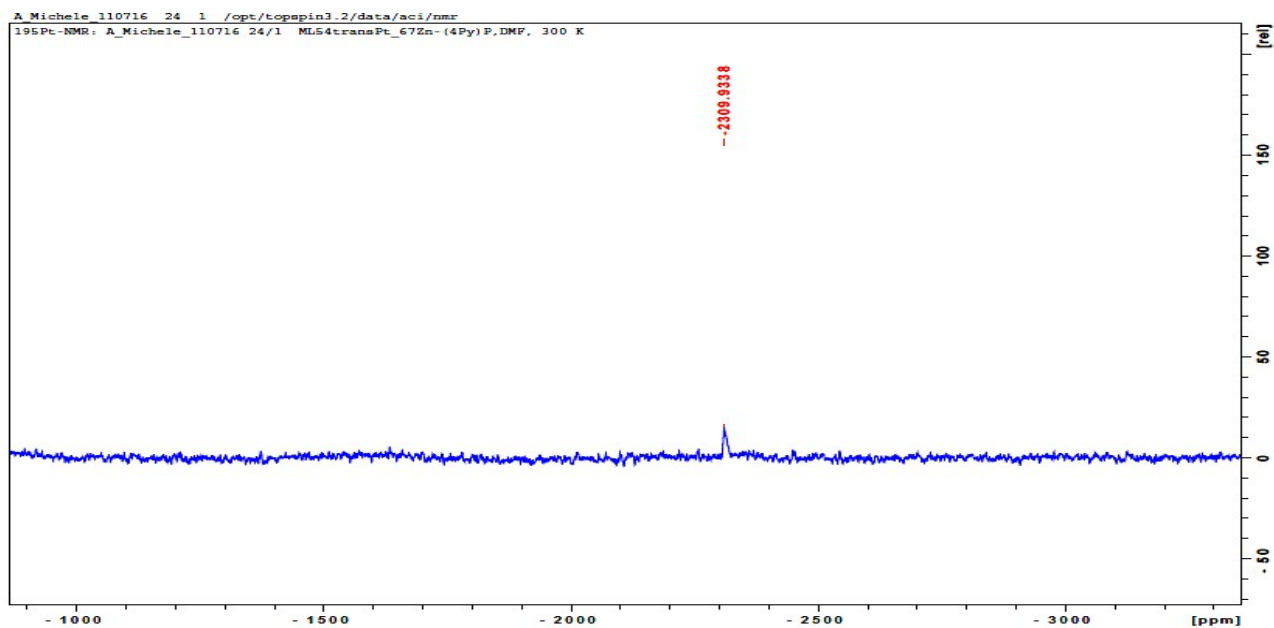


Fig. S11: UV-Vis of **tPt-H₂4PyP**, **tPt-Zn4PyP**, **cPt-H₂4PyP**, **cPt-Zn4PyP**, **dPt-H₂4PyP**, **dPt-Zn4PyP** in DMF

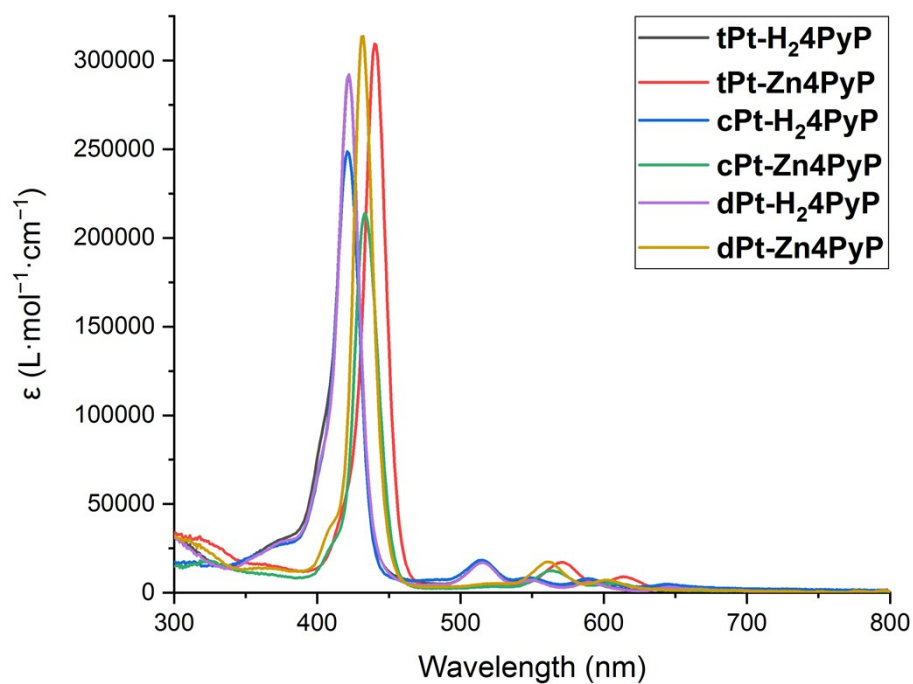
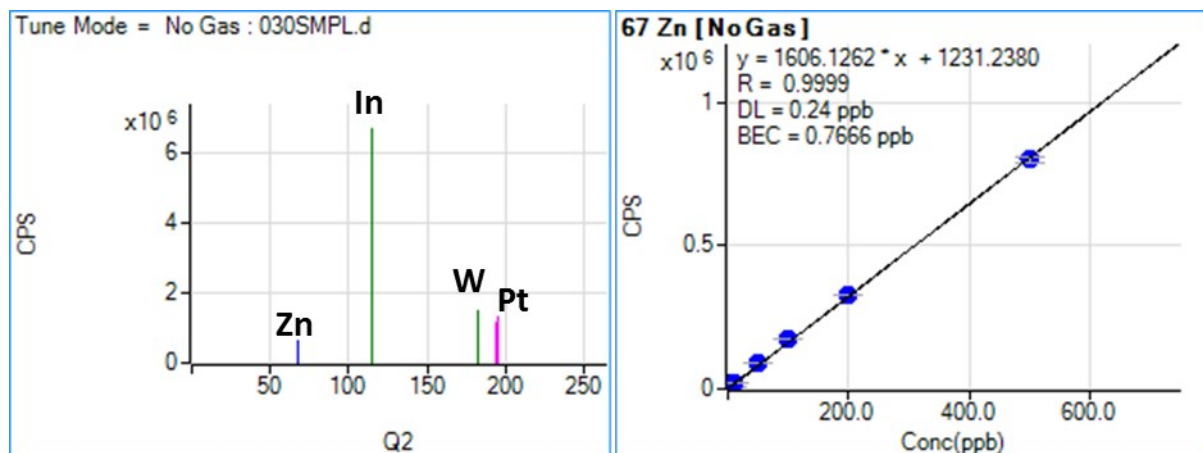
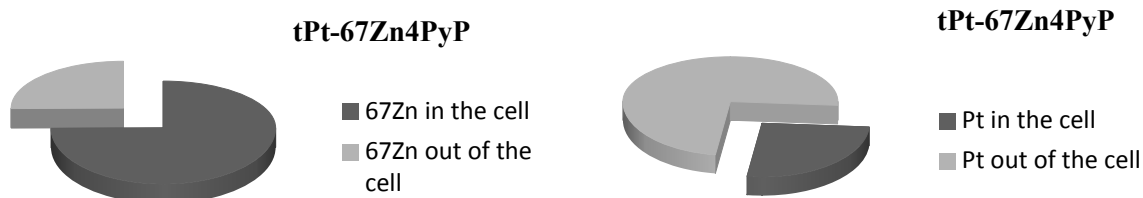


Fig. S12: Example of ^{67}Zn calibration curve in ICP-MS and quantification lines (67, 194 and 195) in no gas mode.



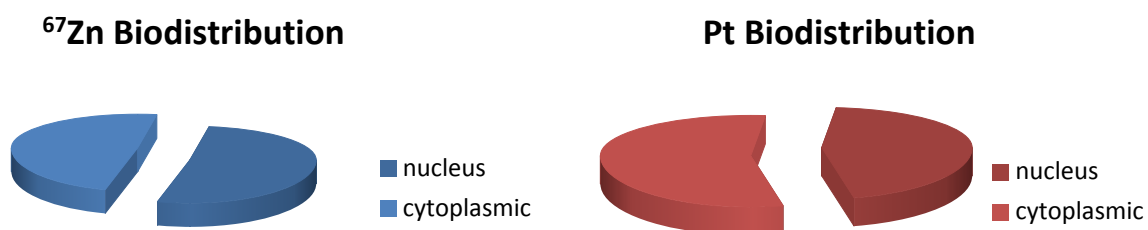
Indium and tungsten were used as internal standard.

Fig. S13: Ratio of intra- and extracellular content of ^{67}Zn and Pt after treatment of HeLa cells with **tPt- $^{67}\text{Zn}4\text{PyP}$**



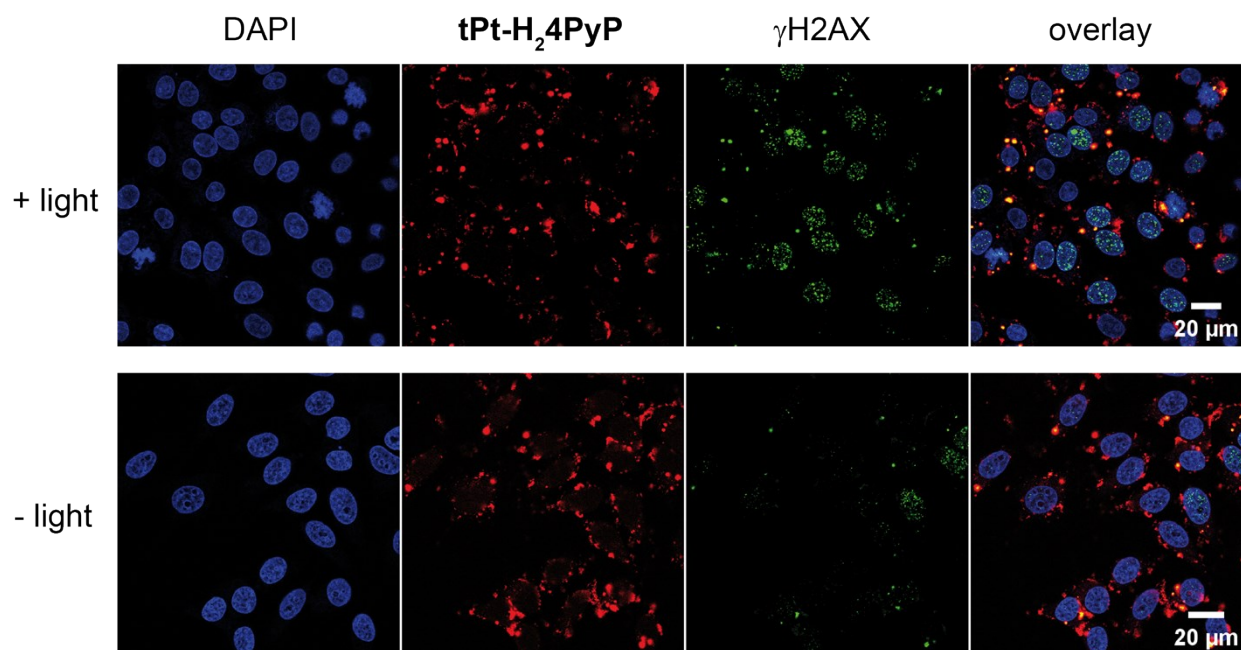
HeLa cells were treated with $10 \mu\text{M}$ of target porphyrin **tPt- $^{67}\text{Zn}4\text{PyP}$** for 4 h. Left panel: Total ^{67}Zn content in the treatment solution (whole pie) and $^{67}\text{zinc}$ content detected in the cell (dark gray part of the pie); Right panel: Total platinum content in the treatment solution (whole pie) and platinum content detected in the cell (dark gray part of the pie).

Fig. S14: ^{67}Zn and Pt biodistribution between nucleus and cytoplasmic fractions after treatment of HeLa cells with **tPt- $^{67}\text{Zn4PyP}$**



HeLa cells were treated with $10\ \mu\text{M}$ **tPt- $^{67}\text{Zn4PyP}$** for 4 h. Left panel: ^{67}Zn biodistribution between nuclear and cytoplasmic fractions; Right panel: Platinum biodistribution between nuclear and cytoplasmic fractions.

Fig. S15: Characterization of DNA damage by γ H2AX induced upon light activation of the photosensitizer **tPt-H₂4PyP**.



Immunofluorescence images of HeLa cells treated with 500 nM of **tPt-H₂4PyP** for 14 h, followed by light irradiation, compared to unirradiated control. Cells were stained with γ H2AX-Alexafluor 594 antibody (green) and DAPI (blue). (**tPt-H₂4PyP**: 458 nm ex., 650-750 nm em.; γ H2AX-Alexafluor 594: 594 nm ex., 610-650 nm em.).

References:

1. a) N. Zhou, Z. C. Sun, Q. Zhou, X. M. Lu and H. W. Shao, *J. Chem. Res.*, 2013, 445-450; b) Q. P. Lin, C. Y. Mao, A. G. Kong, X. H. Bu, X. Zhao and P. Y. Feng, *J. Mater. Chem. A*, 2017, **5**, 21189-21195.
2. M. Babor, P. P. Nievergelt, J. Čejka, V. Zvoniček and B. Spingler, *IUCrJ*, 2019, **6**, 145-151.
3. P. P. Nievergelt, M. Babor, J. Čejka and B. Spingler, *Chem. Sci.*, 2018, **9**, 3716-3722.
4. Rigaku Oxford Diffraction, CrysAlis^{Pro} Software system 1.171.40, Rigaku Corporation, 2019.
5. G. M. Sheldrick, *Acta Cryst.*, 2015, **A71**, 3-8.
6. G. M. Sheldrick, *Acta Cryst.*, 2015, **C71**, 3-8.
7. O. V. Dolomanov, L. J. Bourhis, R. J. Gildea, J. A. K. Howard and H. Puschmann, *J. Appl. Cryst.*, 2009, **42**, 339-341.
8. C. F. Macrae, L. Sovago, S. J. Cottrell, P. T. A. Galek, P. McCabe, E. Pidcock, M. Platings, G. P. Shields, J. S. Stevens, M. Towler and P. A. Wood, *J. Appl. Cryst.*, 2020, **53**, 226-235.
9. M. Huxley, C. Sanchez-Cano, M. J. Browning, C. Navarro-Ranninger, A. G. Quiroga, A. Rodger and M. J. Hannon, *Dalton Trans.*, 2010, **39**, 11353-11364.
10. L. Schneider, M. Larocca, W. Wu, V. Babu, R. Padrutt, E. Slyshkina, C. König, S. Ferrari and B. Spingler, *Photochem. Photobiol. Sci.*, 2019, **18**, 2792-2803.
11. M. S. Meijer, V. S. Talens, M. F. Hilbers, R. E. Kieltyka, A. M. Brouwer, M. M. Natile and S. Bonnet, *Langmuir*, 2019, **35**, 12079-12090.
12. J. B. Verlhac, A. Gaudemer and I. Kraljic, *Nouv. J. Chim.*, 1984, **8**, 401-406.
13. A. Frei, R. Rubbiani, S. Tubafard, O. Blacque, P. Anstaett, A. Felgenträger, T. Maisch, L. Spiccia and G. Gasser, *J. Med. Chem.*, 2014, **57**, 7280-7292.
14. M. M. Bradford, *Anal. Biochem.*, 1976, **72**, 248-254.
15. A. Naik, R. Rubbiani, G. Gasser and B. Spingler, *Angew. Chem. Int. Ed.*, 2014, **53**, 6938-6941.